AAC Journals.ASM.org

The Complete Nucleotide Sequence of the Carbapenem Resistance-Conferring Conjugative Plasmid pLD209 from a *Pseudomonas putida* Clinical Strain Reveals a Chimeric Design Formed by Modules Derived from Both Environmental and Clinical Bacteria

Patricia M. Marchiaro,[a] Luciano Brambilla,[a] Jorgelina Morán-Barrio,[a] Santiago Revale,[c] Fernando Pasteran,[d] Alejandro J. Vila,[b] Alejandro M. Viale,[a] Adriana S. Limansky[a]

Departamento de Microbiología[a] and Departamento de Química Biológica,[b] Instituto de Biología Molecular y Celular de Rosario (IBR, CONICET), Facultad de Ciencias Bioquímicas y Farmacéuticas, Universidad Nacional de Rosario (UNR), Rosario, Argentina; Genomics and Bioinformatics INDEAR, Rosario, Argentina[c]; Servicio Antimicrobianos, Instituto Nacional de Enfermedades Infecciosas-ANLIS Dr. Carlos G. Malbrán, Ciudad Autónoma de Buenos Aires, Buenos Aires, Argentina[d]

The complete sequence of the carbapenem-resistance-conferring conjugative plasmid pLD209 from a *Pseudomonas putida* clinical strain is presented. pLD209 is formed by 3 well-defined regions: an adaptability module encompassing a Tn*402*-like class 1 integron of clinical origin containing bla_{VIM-2} and *aacA4* gene cassettes, partitioning and transfer modules, and a replication module derived from plasmids of environmental bacteria. pLD209 is thus a mosaic of modules originating in both the clinical and environmental (nonclinical) microbiota.

Pseudomonas putida is an opportunistic pathogen generally susceptible to most clinically employed antimicrobial agents and ubiquitous in several niches, including soil, freshwater, and animal surfaces (1). Recently, however, VIM- and IMP-like metallo-β-lactamase (MβL)-containing *P. putida* clinical strains displaying resistance to most β-lactams have been described and proposed to represent MβL gene reservoirs (2–5). This poses a serious challenge to antimicrobial therapy due to the potential role of this environmental species in MβL gene dissemination among human pathogens such as *Pseudomonas aeruginosa* (5, 6). bla_{VIM-2} represents the prevailing gene among *P. putida* MβL producers, a gene generally carried by class 1 integrons (7, 8) (http://www.mbled.uni-stuttgart.de) contained in turn within transposons, with the whole arrangement being rapidly spread over large taxonomic distances by the aid of conjugative plasmids (9, 10). These plasmids are composed of backbone modules, which are responsible for replication, maintenance, and propagation functions, and accessory elements, which contribute adaptive traits to particular hosts within specific environments (10). Uncovering the genetic platform(s) in which *P. putida* bla_{VIM-2} genes are contained may enable us to follow the evolution and dissemination of these elements and eventually provide epidemiological tools to limit the spread of antibiotic resistance among bacterial species inhabiting different niches (11–13). In this context, few data exist on the complete characterization of plasmids carrying bla_{VIM-2} genes in *Pseudomonas* spp (14). We recently reported (3) an unusual class 1 integron carrying bla_{VIM-2} and *aacA4* gene cassettes embedded in a complete Tn*402*-like transposon in a carbapenem-resistant *P. putida* clinical strain, with all elements being carried by a self-transferable plasmid designated pLD209. In this work, we characterized pLD209 on the basis of its complete DNA sequence.

(Part of these results were presented previously [A. Viale, P. Marchiaro, V. Ballerini, T. Spalding, G. Rosignol, A. Vila, and A. Limansky, International Plasmid Biology Conference 2010, Bariloche, Argentina, 6 to 15 November 2010].)

Conjugative plasmid pLD209 (formerly pLD20) was isolated from *P. putida* clinical strain LD209 (3). This plasmid was transferred from *P. putida* LD209 to *Escherichia coli* DH5α with a frequency of 1.8×10^{-3} transconjugants per recipient cell following conventional procedures (3). The complete nucleotide sequence of pLD209 was determined by 454 pyrosequencing (Roche Diagnostics Corporation) at the Instituto de Agrobiotecnología Rosario (INDEAR). Calling and annotation of open reading frames (ORFs) were performed by both ISGA (15) and RAST (16) standard operating procedures for prokaryotic annotation pipelines followed by curation by visual inspection. The complete nucleotide sequence of pLD209 indicated a length of 38,403 bp and 44 predicted ORFs, of which 30 encode proteins with homology to sequences in databases of attributed functions (Table 1). Among the 14 remaining ORFs, 10 have homologs with no reported functions and 4 have no homologs (Table 1). The overall G+C content of pLD209 (56.2%) is significantly lower than that of *P. putida* genomes, which vary between 61.4 and 61.9% (http://www.ncbi.nlm.nih.gov/genome), thus suggesting separate origins.

New proposals for the classification of transmissible plasmids of gammaproteobacterial species are based on the comparisons of the N-terminal 300-amino-acid conserved domain of relaxases encoded by relaxase gene homologs present in these plasmids (17, 18). This approach defined six relaxase families: MOB_F, MOB_H, MOB_Q, MOB_C, MOB_P, and MOB_V (12, 17, 18). Maximum likelihood (ML) phylogenetic analysis (19) using representative amino acid relaxase domains from each of these families (18) indicated a close affiliation of the pLD209 *orf22* product (VirD2) to members

Received 14 November 2013 **Returned for modification** 8 December 2013
Accepted 29 December 2013
Published ahead of print 6 January 2014
Address correspondence to Adriana S. Limansky, limansky@ibr-conicet.gov.ar.
Supplemental material for this article may be found at http://dx.doi.org/10.1128/AAC.02494-13.

doi:10.1128/AAC.02494-13

TABLE 1 Summary of putative coding sequences of pLD209[a]

ORF	Gene	Position (nt)	Direction	Protein length (aa)	Closest relationship		
					Protein/function	Microorganism and/or plasmid	% Amino acid identity[b] (accession number)
orf1	pLD209.1	228–830	+	200	Hypothetical protein	*Xylella fastidiosa*	53.0 (YP_001830948.1)
orf2	*intI1*	1215–2228	−	337	IntI1/integrase	*P. aeruginosa* In*71*	99.0 (CAJ58443.1)
orf3	bla_{VIM-2}	2395–3195	+	266	VIM-2/metallo-β-lactamase	*P. aeruginosa* In*71*	100 (CAJ58444.1)
orf4	*aacA4*	3355–3852	+	165	AacA4/aminoglycoside acetyltransferase	*P. aeruginosa* In*71*	100 (CAJ58445.1)
orf5	*tniC*	4015–4638	−	207	TniC/resolvase	*E. aerogenes* pR751	100 (CAA51178.1)
orf6	*tniQ*	4700–5917	−	405	TniQ/protein involved in trasposition	*E. aerogenes* pR751	100 (CAA51177.1)
orf7	*tniB*	5914–6822	−	302	TniB/protein involved in trasposition	*E. aerogenes* pR751	100 (CAA51176.1)
orf8	*tniA*	6825–8504	−	559	TniA/transposase	*E. aerogenes* pR751	99.0 (CAA51175.1)
orf9	*tnpC*	8773–9135	+	120	TnpC/TnpA repressor protein	*P. syringae* pv. tomato T1	85.0 (EEB56639.1)
orf10	pLD209.10	9138–9365	+	75	Hypothetical protein	*P. syringae* pv. tomato T1	88.0 (EEB56638.1)
orf11	pLD209.11	9534–9719	−	61	Hypothetical protein	*P. syringae*	66.0 (WP_016567456)
orf12	pLD209.12	9819–10031	−	70	Hypothetical protein	*P. syringae* pv. maculicola	23.0 (YP_025629)
orf13	pLD209.13	10181–10348	−	55	Hypothetical protein	*P. syringae*	54.0 (WP_003425135)
orf14	*repA*	10965–12212	+	415	RepA/replicase	Uncultured bacterium pRSB101	66.0 (CAG27822.1)
orf15	*trfB*	12490–12813	+	107	TrfB/transcriptional represor protein	*X. albilineans* plasmIII	56.2 (CAZ15854.1)
					KorA/transcriptional represor protein	*A. caviae* pFBAOT6	35.6 (CAG15055.1)
orf16	*parA*	12810–13616	+	268	ParA/plasmid partitioning protein	*X. albilineans* plasmIII	56.3 (CAZ15823.1)
					IncC/ParA family ATPase	*A. caviae* pFBAOT6	33.5 (CAG15056.1)
orf17	*parB*	13609–14673	+	354	ParB/ParB-like partition protein	*X. albilineans* plasmIII	37.6 (CAZ15824.1)
					KorB/transcription represor protein	*A. caviae* pFBAOT6	31.5 (CAG15057.1)
orf18	pLD209.18	14735–14923	+	62	Hypothetical protein with no significant database matches		
orf19	pLD209.19	15106–15384	+	92	Hypothetical protein with no significant database matches		
orf20	*mpR*	15975–16685	−	236	Metalloprotease	*X. albilineans* plasmIII	64.5 (CAZ15825.1)
					MpR/metallopeptidase	*A. caviae* pFBAOT6	54.5 (CAG15059.1)
orf21	*mobC*	17256–17813	+	185	MobC/mobilization protein	*X. albilineans* plasmIII	49.7 (CAZ15826.1)
					MobC/mobilization protein	*A. caviae* pFBAOT6	30.3 (CAG15060.1)
orf22	*virD2*	17800–18831	+	343	DNA relaxase-nickase protein	*X. albilineans* plasmIII	59.6 (CAZ15827.1)
					VirD2/relaxase	*A. caviae* pFBAOT6	42.6 (CAG15061.1)
orf23	pLD209.23	18911–19162	+	83	Hypothetical protein with no significant database matches		
orf24	pLD209.24	19957–20166	+	69	Hypothetical protein	*P. syringae*	63.0 (YP_006964224)
orf25	pLD209.25	20375–21010	+	211	Resolvase	*P. syringae* pv. pisi	55.7 (EGH44160.1)
orf26	pLD209.26	21063–21263	+	66	Hypothetical protein with no significant database matches		
orf27	pLD209.27	21472–21705	+	77	Hypothetical protein	Uncultured bacterium	52.0 (AGH89230.1)
orf28	pLD209.28	21984–22364	+	126	Hypothetical protein	*P. fluorescens*	54.0 (WP_019692597)
orf29	pLD209.29	22412–23041	−	209	Lytic transglycosylase protein	*X. albilineans* plasmIII	61.0 (CAZ15836.1)
orf30	*traC4*	23038–24942	−	634	DNA primase	*X. albilineans* plasmIII	49.8 (CAZ15837.1)
					TraC4/DNA primase	*A. caviae* pFBAOT6	33.0 (CAG15064.1)
orf31	*virD4*	25223–27133	−	636	VirD4/conjugal transfer protein	*X. albilineans* plasmIII	61.6 (CAZ15838.1)
						A. caviae pFBAOT6	41.5 (CAG15065.1)
orf32	*virB11*	27143–28189	−	348	VirB11/conjugal transfer protein	*X. albilineans* plasmIII	45.4 (CAZ15839.1)
						A. caviae pFBAOT6	38.0 (CAG15066.1)
orf33	*virB10*	28186–29394	−	402	VirB10/conjugal transfer protein	*X. albilineans* plasmIII	38.0 (CAZ15840.1)
						A. caviae pFBAOT6	35.4 (CAG15067.1)
orf34	*virB9*	29397–30206	−	269	VirB9/conjugal transfer protein	*X. albilineans* plasmIII	46.0 (CAZ15841.1)
						A. caviae pFBAOT6	32.0 (CAG15068.1)
orf35	*virB8*	30209–31102	−	297	VirB8/conjugal transfer protein	*X. albilineans* plasmIII	44.8 (CAZ15842.1)
						A. caviae pFBAOT6	27.0 (CAG15069.1)
orf36	*virB7*	31102–31287	−	61	VirB7/conjugal transfer protein	*X. albilineans* plasmIII	61.0 (CAZ15843.1)
					Lipoprotein	*A. caviae* pFBAOT6	33.0 (CAG15070.1)
orf37	*virB6*	31420–32370	−	316	VirB6/conjugal transfer protein	*X. albilineans* plasmIII	52.7 (CAZ15844.1)
						A. caviae pFBAOT6	26.0 (CAG15071.1)
orf38	*virB5*	32581–33312	−	243	VirB5/conjugal transfer protein	*X. albilineans* plasmIII	50.0 (CAZ15846.1)
						A. caviae pFBAOT6	30.0 (CAG15073.1)
orf39	*virB4*	33309–35744	−	811	VirB4/conjugal transfer protein	*X. albilineans* plasmIII	60.0 (CAZ15847.1)
						A. caviae pFBAOT6	41.5 (CAG15074.1)
orf40	*virB3*	35741–36109	−	122	VirB3/conjugal transfer protein	*X. albilineans* plasmIII	65.5 (CAZ15848.1)
						A. caviae pFBAOT6	46.2 (CAG15075.1)
orf41	*virB2*	36137–36460	−	107	VirB2/Conjugal transfer protein	*X. albilineans* plasmIII	50.9 (CAZ15849.1)
						A. caviae pFBAOT6	32.0 (CAG15076.1)
orf42	pLD209.42	36438–36806	−	122	Hypothetical protein	*X. albilineans* plasmIII	48.2 (CAZ15850.1)
						A. caviae pFBAOT6	38.5 (CAG15077.1)
orf43	pLD209.43	36826–37386	−	186	Hypothetical protein	*X. albilineans* plasmIII	35.0 (CAZ15851.1)
orf44	pLD209.44	37474–38403	−	309	Protein with toprim domain	*X. albilineans* plasmIII	67.0 (CAZ15852.1)

[a] nt, nucleotides; aa, amino acids.

[b] The BLASTp algorithm was used to search for protein similarities in databases. The criteria used to define amino acid sequence homology to the sequences indicated by the corresponding accession numbers were ≥25% identity at the amino acid level and ≥50% coverage of protein length (14).

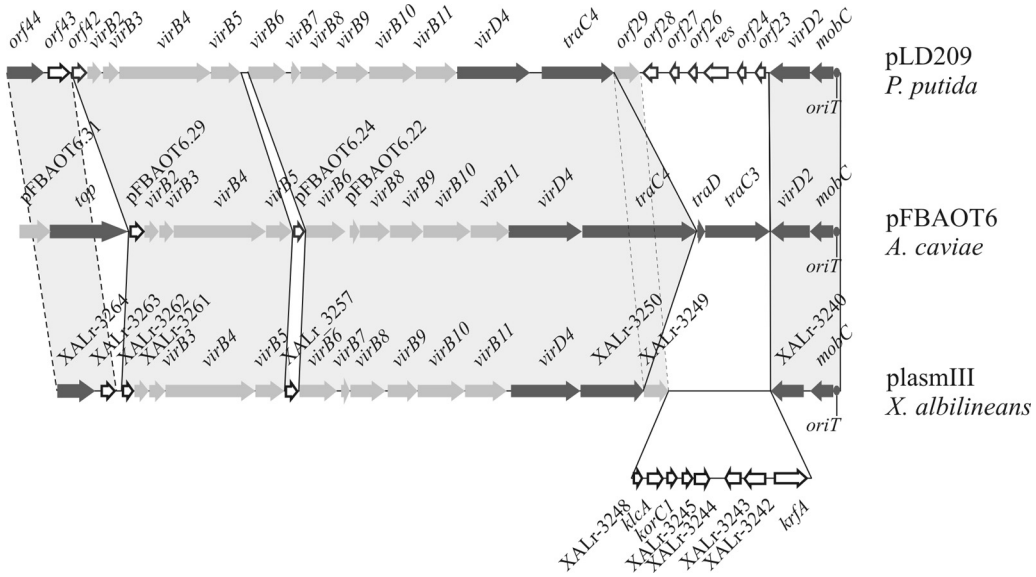

FIG 1 Comparative analysis of the transfer modules of pLD209, pFBAOT6, and plasmIII. For clarity, linear genetic maps of pLD209 (21,256 bp), pFBAOT6 from *Aeromonas caviae* (20,956 bp; CR376602.1) (20), and plasmIII from *X. albilineans* (21,504 bp; FP340277) (25) are shown. The arrows indicate the direction of transcription of the different genes. The predicted mating pair formation (Mpf) genes are shown in gray. The predicted DNA transfer region (DTR) genes are shown in dark gray. The positions of the *oriT*s are indicated by ovals. ORFs encoding hypothetical proteins or proteins which are not common among the three plasmids are shown by white arrows. The vertical gray areas between the three plasmids indicate similar gene functions in all cases. The vertical gray areas bordered by dashed lines indicate similar gene functions among pLD209 and plasmIII. See Table 1 for details.

of the MOB_P family (not shown). A subsequent ML phylogenetic tree constructed by using relaxase domains from plasmids of the MOB_P subfamilies as well as alignments of conserved relaxase motifs (18) indicated the closest affiliation of pLD209 VirD2 with its homologs of the MOB_{P4} subfamily (see Fig. S1 in the supplemental material). The MOB_{P4} relaxase clade is extensive and includes a subclade formed by proteins from IncU conjugative plasmids such as pFBAOT6 and RA3 from *Aeromonas* spp. (17, 20, 21). Another MOB_{P4} subclade is defined by relaxases encoded by broad-host-range (BHR) plasmids such as pIPO2 (22), pSB102 (23), and pXF51 (24) from soil bacteria. Sequence comparisons of VirD2 proteins from all of the above plasmids indicated the highest identity of the protein encoded by pLD209 with that encoded by pFBAOT6 (42.6%) (Table 1). All IncU plasmids have a common backbone/core region encoding replication, maintenance, and transfer modules but differ in a variable region containing the resistance-determining genes (21). We thus compared first the arrangement and sequences of the core regions of pLD209 and pFBAOT6 (Fig. 1 and 2; Table 1). In addition, we conducted a parallel search in databases of each predicted protein product encoded by pLD209 ORFs (Table 1) for best matches. The results are as follows.

(i) Conjugative transfer functions. A pLD209 region spanning approximately 9,300 bp comprising 10 genes from *orf41* to *orf32* (Table 1) most closely resembles the *virB2* to *virB11* gene clusters from *Xanthomonas albilineans* plasmIII (25) and *Aeromonas caviae* pFBAOT6 (20) involved in mating pair formation (Fig. 1 and 3). Similar to the *virB* clusters of these plasmids, pLD209 also lacks a well-defined *virB1*, although a putative homolog, *orf29*, was identified downstream of the *virB* cluster (Fig. 1). The *orf29* product, similar to other VirB1-like proteins (20), contains a lytic transglycosylase domain promoting localized peptidoglycan lysis during pilus assembly (Table 1). It is noteworthy that a putative lytic transglycosylase gene (XALr_3249) is also located in *X. albilineans* plasmIII at a position similar to that of *orf29* (Fig. 1).

The pLD209 DNA transfer region (DTR) comprises around 7,000 bp and includes *orf21*, *orf22*, *orf30*, *orf31*, and *orf44* (Table 1;

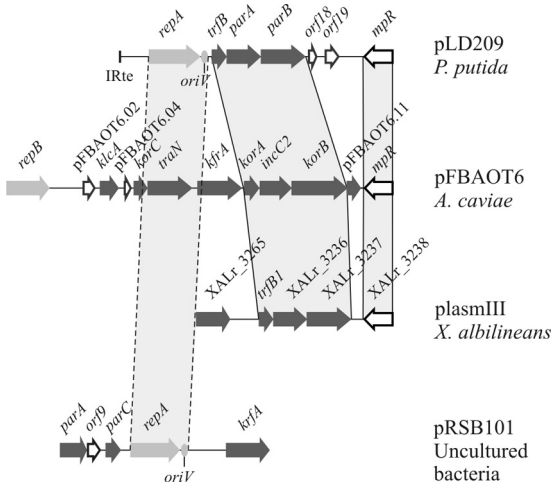

FIG 2 Comparative analysis of the replication and partitioning modules of pLD209, pFBAOT6, plasmIII, and pRSB101. For clarity, linear genetic maps of pLD209 (5,892 bp), pFBAOT6 from *A. caviae* (9,547 bp; CR376602.1) (20), plasmIII from *X. albilineans* (3,192 bp; FP340277) (25), and pRSB101 (5,034 bp; AJ698325.1) (26) are shown. The arrows indicate the direction of transcription. Partitioning genes are indicated in dark gray. The *repA* genes are indicated in gray, and *oriV* is shown by ovals. ORFs encoding hypothetical proteins and genes displaying functions not associated with a specific module (e.g., *mpr* homologs) are shown by white arrows. The vertical gray areas shown between pLD209, pFBAOT6, and plasmIII indicate similar gene functions. The vertical gray area bordered by dashed lines indicates similar *repA* genes and *oriV* regions among pLD209 and pRSB101. See Table 1 for details.

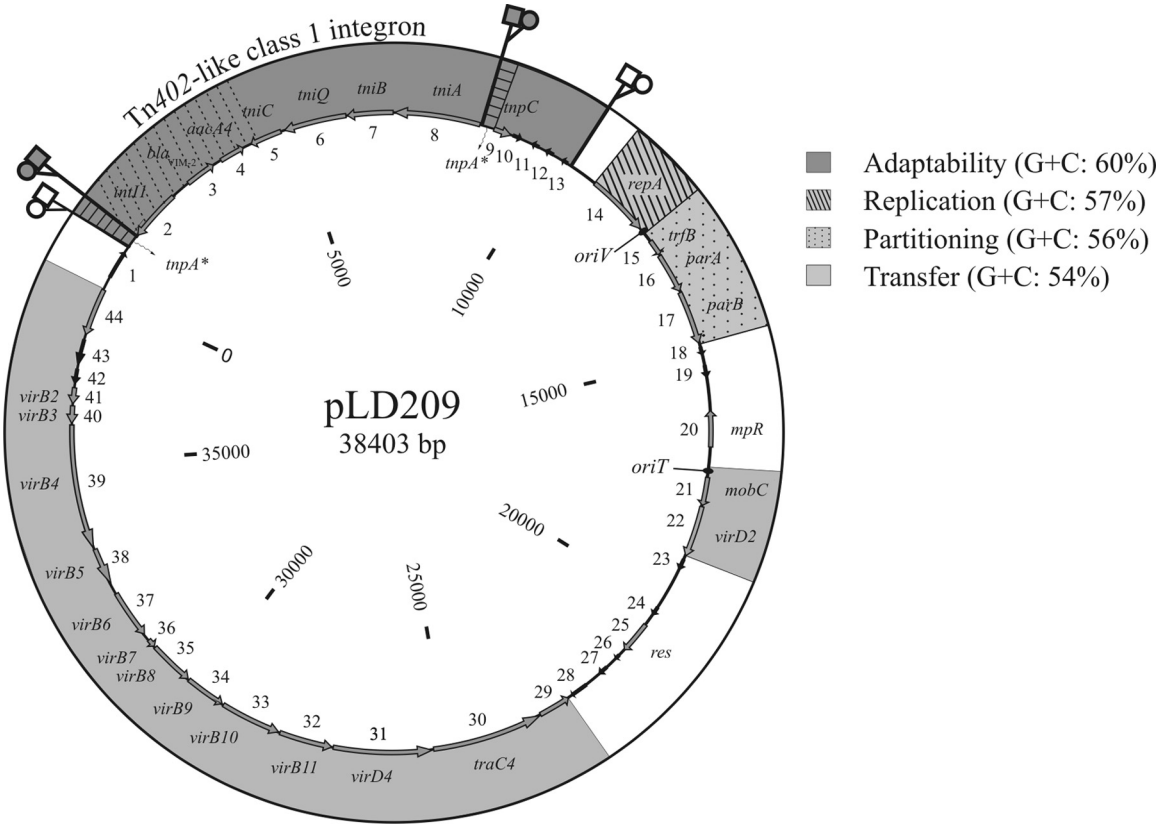

FIG 3 Genetic map of pLD209. ORFs are shown in the inner circle, with the direction of transcription indicated by arrows. Black arrows point to ORFs that have no homologs in databases or whose functions are unknown. The modular structure of the plasmid is indicated by shades of gray. ORF numbers and their corresponding predicted functions are indicated on the inner and outer circles, respectively (see also Table 1). The *oriV* and *oriT* sites are marked. The target site of Tn*402*-like class 1 integron (*tnpA**) is indicated in the adaptability module by horizontal lines; the initial inverted repeat (IRi; GQ857074) and the terminal inverted repeat (IRt; GQ857074) bracketing Tn*402*-like class 1 integron are indicated by dark gray squares; and the initial and terminal direct repeats (DRi and DRt) are indicated by dark gray circles. The white squares indicate the external IRs (IRie and IRte; 5′-GGGGGTGTAAGCCGGAACCCCAGAAAATTCCGTC-3′), and the white circles indicate the external direct repeats (DRie and DRte; 5′-TATTC-3′). The vertical dotted lines region inside Tn*402*-like class 1 integron encompassing *intI1*, bla_{VIM-2}, *aacA4*, and the 3′ end of *tniC* correspond to the In*71* integron reported for *P. aeruginosa* clinical strains (33).

Fig. 1 and 3). The *orf21* product displays the highest similarity to MobC (accessory mobilization protein) from *X. albilineans* plasmIII (49.7%) and *A. caviae* pFBAOT6 (30.3%) (Table 1). The *orf22* product has the highest similarity to a nickase from *X. albilineans* plasmIII (59.6%) and to the VirD2 relaxase from *A. caviae* pFBAOT6 (42.6%). Notably, in pLD209, plasmIII, and pFBAOT6, the corresponding relaxase genes are transcribed in directions opposite that of the DTR genes *traC4*, *virD4*, and *orf44* (Fig. 1). The *orf30* product, in turn, shows the highest similarity to TraC4 DNA primases from *X. albilineans* plasmIII (49.8%) and *A. caviae* pFBAOT6 (33.0%). The *orf31* product shows the highest similarity to the VirD4 conjugal transfer proteins from *X. albilineans* plasmIII (61.6%) and *A. caviae* pFBAOT6 (41.5%). Finally, *orf44*, which is located upstream of the pLD209 *virB* cluster (Fig. 1), encodes a putative protein with a Toprim domain common to topoisomerases and exhibits 67.0% identity to the XALr_3264 topoisomerase from *X. albilineans* plasmIII (Table 1). No sequence homolog was identified in *A. caviae* pFBAOT6, although a predicted topoisomerase gene is located in pFBAOT6 in a position similar to that in both pLD209 and plasmIII (Fig. 1) and separated from the other transfer genes by the mating pair formation (Mpf) complex. The latter feature is common to the MOB_{P4} plasmid subfamily, which includes the IncU plasmid group (20, 21) and environmental BHR plasmids such as pIPO2, pSB102, and pXF51 (22–24). In fact, the location of the topoisomerase gene upstream of *virB2* that is common to pLD209, pFBAOT6, and BHR plasmids (Fig. 1) is different from that in members of the IncP group, such as RP4, in which the corresponding genes are located in the DTR (21). The common location of these genes in *P. putida* pLD209, *X. albilineans* plasmIII, and *A. caviae* pFBAOT6, and the opposite transcription of *virD2* with respect to the other DTR genes (Fig. 1), are also typical features of the MOB_{P4} plasmid subfamily (17, 20–24).

The origin of transfer of pLD209 was located immediately upstream of *mobC* (Fig. 1) on the basis of sequence homology with *oriT* sequences of pFBAOT6, pIPO2, pSB102, and pXF51 (20). The TATCCTG ↓ C nickase recognition sequence is identical to that of environmental plasmids pXF51, pIPO2, and pSB102 (22) and very similar to the AATCCTG ↓ C motif of pFBAOT6 and pRA3 (20). Our analysis also identified the *oriT* region of *X. albilineans* plasmIII in a position similar to that in pLD209 (Fig. 1).

(ii) Stability module. pLD209 *orf15*, *orf16*, and *orf17*, encoding putative partitioning proteins, are clustered in a region downstream of *orf14*, a putative replicase gene (Table 1; Fig. 2). The three genes are in the same organization in pLD209 as their homologs in *X. albilineans* plasmIII and *A. caviae* pFBAOT6

(Table 1; Fig. 2). Notably, and opposite to pLD209 and plasmIII, pFBAOT6 maintenance and partitioning functions comprise five additional ORFs located downstream of the *rep* gene (Fig. 2). An *mpr* gene encoding a putative metalloprotease (MpR) displaying homology to XALr_3238 from *X. albilineans* plasmIII and MpR from pFBAOT6 (Table 1; Fig. 2) is located upstream of the *oriT* region (Fig. 3).

(iii) Replication functions. The pLD209 replication module spans approximately 1,500 bp and encompasses *orf14* and the *oriV* region (Fig. 3). The *orf14* product shows high similarity to pRSB101 RepA (66.0%) and no detectable homology to pFBAOT6 RepB (Table 1; Fig. 2). This argues for a separate origin for the replication regions of pLD209 and pFBAOT6, contrary to the case of the corresponding transfer and stability modules.

The *oriV* of pLD209 was located downstream of *repA* (Fig. 2) based on the similarity of two repeat sequences (R1 and R2), the DnaA box, and a 52-bp A+T-rich (73.0%) region to those reported for pRSB101 (26). Similarly to pRSB101, pLD209 R2 has three copies of the CCAGG motif (two in one strand and the other in the complementary strand) and a TTAGCCAC DNA box located in the same strand as this third CCAGG copy. In contrast, pLD209 R1 shows a lower number (three) of TAGCC repetitions.

(iv) Adaptability module. The adaptability module region spans approximately 9,500 bp and bears a complete Tn*402*-like class 1 integron (3) carrying a class 1 integron with bla_{VIM-2} and *aacA4* gene cassettes (Fig. 3). Concatenation of 88 bp upstream of the initial inverted repeat (IRi) (positions 925 to 1,012) and 112 bp downstream of the terminal inverted repeat (IRt) (positions 8,651 to 8,762) of Tn*402*-like class 1 integron uncovered a 200-bp fragment displaying high sequence similarity (60.0%) to the 3′ end of *tnpA*, coding for the Tn*3* family transposase present in *Pseudomonas syringae* ISYps3 (NZ_GG700365.1). A GTTTT duplication bracketing the two IRs mentioned above provided strong additional evidence for a transposition event, with all evidence suggesting that Tn*402*-like class 1 integron targets a Tn*3*-like *tnpA* gene in the pLD209 precursor.

It is worth noting that *orf9* encoding a protein displaying 85.0% identity with the TnpA repressor TnpC is located downstream of the truncated *tnpA* in pLD209 (Table 1; Fig. 3). Moreover, a 5-bp TATTC external direct repeat (DRie) sequence immediately followed by a 34-bp external inverted repeat (IRie) exhibiting 97.0% identity with the IR of a Tn*5501*-like transposon of *Pseudomonas savastanoi* (FR820585.1) is located upstream of the insertion site of the Tn*402*-like integron (Fig. 3). These two sequences are exactly repeated upstream of *orf13* at the opposite end of the transposon (IRte and DRte, respectively) (Fig. 3). Moreover, the presence of external DRie and DRte bracketing the boundaries of this adaptability module strongly suggest TATTC target duplications associated with an earlier transposition event.

Our results above showed that pLD209 carries vestiges of a Tn*3*-like transposon, including a truncated *tnpA*, a complete *tnpC* repressor gene, and accompanying inverted repeats IRie and IRte (Fig. 3). It is therefore tempting to speculate that the *tnpA* gene constituted the original target of Tn*402*-like class 1 integron in an aboriginal Tn*3*-like element and that further deletions and rearrangements eliminated the original *res* and resolvase gene regions (27–29), thus generating the adaptability module depicted in Fig. 3. In this context, Tn*3*-like elements such as Tn*4652* have been described in the chromosome of a *P. putida* strain encompassing only *tnpA* and *tnpC* genes bracketed by IRs (30), a situation resembling the proposed precursor element of the arrangement now found in pLD209. Thus, we provide in this work further evidences of mobile genetic elements inserting into one another, thus generating novel antimicrobial resistance-conferring platforms (31, 32). Additional studies are certainly necessary to determine whether the mobilizable Tn*402*-like class 1 integron element present in pLD209 has definite limits in the internal IRs or whether it may additionally extend also to the external IRs, alternatives that are in any case not mutually exclusive.

To our knowledge, pLD209 represents the first completely sequenced *P. putida* conjugative plasmid carrying bla_{VIM-2} composed of different modules derived from nonclinical (environmental) and clinical bacterial sources. Thus, the partitioning and transfer modules of pLD209 are closely related to equivalent modules found in the IncU plasmid pFBAOT6 from an *A. caviae* strain isolated from hospital effluents (20, 21) and BHR plasmids from plant-associated bacteria (22–24). A similar modular architecture is also shared by plasmIII of the plant pathogen *X. albilineans* (Fig. 1 and 2). Notably, although the partitioning and transfer modules of all the above plasmids are homologous, their replication modules show significant differences (Fig. 2). Thus, the pLD209 replication module is similar to that of multiresistance-conferring plasmid pRSB101 obtained from community bacteria isolated from a wastewater treatment facility (26). In turn, the adaptability module most probably derives from a different origin than the other modules, as suggested from the fluctuations in G+C contents along the pLD209 sequence (Fig. 3). In this context, we noted previously (3) that the 5′ region of the Tn*402*-like integron is identical to a class 1 integron found in carbapenem-resistant *P. aeruginosa* clinical strains (33), thus suggesting the clinical microbiota as its most recent source. Whether this bla_{VIM-2} module was directly provided by clinical bacteria or indirectly through environmental bacteria in contact with hospital effluents, representing reservoirs of clinically relevant MβL genes (11, 32), requires more comprehensive sequence analyses.

P. putida is well adapted to nosocomial settings and represents a reservoir of genetic platforms bearing MβLs genes such as pLD209, a plasmid capable of being mobilized not only to other pseudomonads but also to enterobacterial species (3). Moreover, we have found this plasmid in genetically distinct *P. putida* clinical strains isolated from different hospitals in Argentina over extended time periods, as described previously (P. Marchiaro et al., presented at the XIII Congreso Argentino de Microbiología, Buenos Aires, Argentina, 23 to 26 September 2013). The possibility that *P. putida* bridges the environmental and clinical mobilomes certainly deserves further studies.

Nucleotide sequence accession number. The pLD209 sequence and annotation described here have been deposited in the GenBank database under accession number KF840720.

ACKNOWLEDGMENTS

We are grateful to the personnel of the Bacteriology Service, Hospital Provincial, Rosario, Argentina, for kindly providing *P. putida* clinical strains.

P.M. and A.L. are researchers of the National University of Rosario. J.M-B., A.M.V. and A.J.V. are staff members of CONICET. L.B. is a former fellow of CONICET. F.P. is a researcher of the Malbrán Institute, Buenos Aires. S.R. is a staff member of Genomics and Bioinformatics INDEAR. No conflicts of interest are declared.

This work was supported by grants from the Agencia Nacional de Promoción Científica y Tecnológica (ANPCyT, Argentina); Consejo Na-

cional de Investigaciones Científicas y Técnicas (CONICET); Ministerio de Salud, Provincia de Santa Fe; and Secretaría de Salud Pública, Municipalidad de Rosario.

REFERENCES

1. **Aumeran C, Paillard C, Robin F, Kanold J, Baud O, Bonnet R, Souweine B, Traore O.** 2007. *Pseudomonas aeruginosa* and *Pseudomonas putida* outbreak associated with contaminated water outlets in an oncohaematology paediatric unit. J. Hosp. Infect. **65:**47–53. http://dx.doi.org/10.1016/j.jhin.2006.08.009.
2. **Almuzara M, Radice M, Gárate N de, Kossman A, Cuirolo A, Santella G, Famiglietti A, Gutkind G, Vay V.** 2007. VIM-2–producing *Pseudomonas putida*, Buenos Aires. Emerg. Infect. Dis. **13:**668–669. http://dx.doi.org/10.3201/eid1304.061083.
3. **Marchiaro P, Viale AM, Ballerini V, Rossignol G, Vila AJ, Limansky A.** 2010. First report of a Tn*402*-like class 1 integron carrying bla_{VIM-2} in *Pseudomonas putida* from Argentina. J. Infect. Dev. Ctries. **4:**412–416. http://dx.doi.org/10.3855/jidc.1012.
4. **Juan C, Zamorano L, Mena A, Albertí S, Pérez JL, Oliver A.** 2010. Metallo-β-lactamase-producing *Pseudomonas putida* as a reservoir of multidrug resistance elements that can be transferred to successful *Pseudomonas aeruginosa* clones. J. Antimicrob. Chemother. **65:**474–478. http://dx.doi.org/10.1093/jac/dkp491.
5. **Carvalho-Assef AP, Gomes MZ, Silva AR, Werneck L, Rodrigues CA, Souza MJ, Asensi MD.** 2010. IMP-16 in *Pseudomonas putida* and *Pseudomonas stutzeri*: potential reservoirs of multidrug resistance. J. Med. Microbiol. **59:**1130–1131. http://dx.doi.org/10.1099/jmm.0.020487-0.
6. **Crowder MW, Spencer J, Vila AJ.** 2006. Metallo-β-lactamases: novel weaponry for antibiotic resistance in bacteria. Acc. Chem. Res. **39:**721–728. http://dx.doi.org/10.1021/ar0400241.
7. **Poirel L, Cabanne L, Collet L, Nordmann P.** 2006. Class II transposon-borne structure harboring metallo-β-lactamase gene bla_{VIM-2} in *Pseudomonas putida*. Antimicrob. Agents Chemother. **50:**2889–2891. http://dx.doi.org/10.1128/AAC.00398-06.
8. **Toleman MA, Vinodh H, Sekar U, Kamat V, Walsh TR.** 2007. bla_{VIM-2}-harboring integrons isolated in India, Russia, and the United States arise from an ancestral class 1 integron predating the formation of the 3′ conserved sequence. Antimicrob. Agents Chemother. **51:**2636–2638. http://dx.doi.org/10.1128/AAC.01043-06.
9. **Smillie C, Garcillán-Barcia P, Francia MV, Rocha E, de la Cruz F.** 2010. Mobility of plasmids. Microbiol. Mol. Biol. Rev. **74:**434–452. http://dx.doi.org/10.1128/MMBR.00020-10.
10. **Norman A, Hansen LH, Sørensen SJ.** 2009. Conjugative plasmids: vessels of the communal gene pool. Philos. Trans. R. Soc. B **364:**2275–2289. http://dx.doi.org/10.1098/rstb.2009.0037.
11. **Cantón R.** 2009. Antibiotic resistance genes from the environment: a perspective through newly identified antibiotic resistance mechanisms in the clinical setting. Clin. Microbiol. Infect. Dis. **15:**20–25. http://dx.doi.org/10.1111/j.1469-0691.2008.02679.x.
12. **Garcillán-Barcia MP, Alvarado A, de la Cruz F.** 2011. Identification of bacterial plasmids based on mobility and plasmid population biology. FEMS Microbiol. Rev. **35:**936–956. http://dx.doi.org/10.1111/j.1574-6976.2011.00291.x.
13. **Perry JA, Wright GD.** 2013. The antibiotic resistance "mobilome": searching for the link between environment and clinic. Front. Microbiol. **4:**138. http://dx.doi.org/10.3389/fmicb.2013.00138.
14. **Bonnin RA, Poirel L, Nordmann P, Eikmeyer FG, Wibberg D, Pühler A, Schlüter AJ.** 2013. Complete sequence of broad-host range plasmid pNOR-2000 harbouring the metallo-β-lactamase gene bla_{VIM-2} from *Pseudomonas aeruginosa*. J. Antimicrob. Chemother. **68:**1060–1065. http://dx.doi.org/10.1093/jac/dks526.
15. **Hemmerich C, Buechlein A, Podicheti R, Revanna KV, Dong Q.** 2010. An Ergatis-based prokaryotic genome annotation web server. Bioinformatics **26:**1122–1124. http://dx.doi.org/10.1093/bioinformatics/btq090.
16. **Aziz RK, Bartels D, Best AA, DeJongh M, Disz T, Edwards RA, Formsma K, Gerdes S, Glass EM, Kubal M, Meyer F, Olsen GJ, Olson R, Osterman AL, Overbeek RA, McNeil LK, Paarmann D, Paczian T, Parrello B, Pusch GD, Reich C, Stevens R, Vassieva O, Vonstein V, Wilke A, Zagnitko O.** 2008. The RAST server: rapid annotations using subsystems technology. BMC Genomics **9:**75. http://dx.doi.org/10.1186/1471-2164-9-75.
17. **Garcillán-Barcia MP, Francia MV, de la Cruz F.** 2009. The diversity of conjugative relaxases and its application in plasmid classification. FEMS Microbiol. Rev. **33:**657–687. http://dx.doi.org/10.1111/j.1574-6976.2009.00168.x.
18. **Alvarado A, Garcillán-Barcia MP, de la Cruz F.** 2012. A degenerate primer MOB typing (DPMT) method to classify gamma-proteobacterial plasmids in clinical and environmental settings. PLoS One **7:**e40438. http://dx.doi.org/10.1371/journal.pone.0040438.
19. **Felsenstein J.** 1989. PHYLIP—phylogeny inference package (version 3.2). Cladistics **5:**164–166.
20. **Rhodes G, Parkhill J, Bird C, Ambrose K, Jones MC, Huys G, Swings J, Pickup RW.** 2004. Complete nucleotide sequence of the conjugative tetracycline resistance plasmid pFBAOT6, a member of a group of IncU plasmids with global ubiquity. Appl. Environ. Microbiol. **70:**7497–7510. http://dx.doi.org/10.1128/AEM.70.12.7497-7510.2004.
21. **Kulinska A, Czeredys M, Hayes F, Jagura-Burdzy G.** 2008. Genomic and functional characterization of the modular broad-host-range RA3 plasmid, the archetype of the IncU group. Appl. Environ. Microbiol. **74:**4119–4132. http://dx.doi.org/10.1128/AEM.00229-08.
22. **Tauch A, Schneiker AS, Selbitschka W, Puhler A, Van Overbeek LS, Smalla K, Thomas CM, Bailey MJ, Forney LJ, Weightman A, Ceglowski P, Pembroke T, Tietze E, Schroder G, Lanka E, Van Elsas JD.** 2002. The complete nucleotide sequence and environmental distribution of the cryptic, conjugative, broad-host-range plasmid pIPO2 isolated from bacteria of the wheat rhizosphere. Microbiology **148:**1637–1653. http://mic.sgmjournals.org/content/148/6/1637.long.
23. **Schneiker S, Keller M, Droge M, Lanka E, Puhler A, Selbitschka W.** 2001. The genetic organization and evolution of the broad host range mercury resistance plasmid pSB102 isolated from a microbial population residing in the rhizosphere of alfalfa. Nucleic Acids Res. **29:**5169–5181. http://dx.doi.org/10.1093/nar/29.24.5169.
24. **Marques MV, da Silva AM, Gomes SL.** 2001. Genetic organization of plasmid pXF51 from the plant pathogen *Xylella fastidiosa*. Plasmid **45:**184–199. http://dx.doi.org/10.1006/plas.2000.1514.
25. **Pieretti I, Royer M, Barbe V, Carrere S, Koebnik R, Cociancich S, Couloux A, Darrasse A, Gouzy J, Jacques MA, Lauber E, Mangenot CS, Poussier S, Segurens B, Szurek B, Verdier V, Arlat M, Rott P.** 2009. The complete genome sequence of *Xanthomonas albilineans* provides new insights into the reductive genome evolution of the xylem-limited *Xanthomonadaceae*. BMC Genomics **10:**616. http://dx.doi.org/10.1186/1471-2164-10-616.
26. **Szczepanowski R, Krahn I, Linke B, Goesmann A, Puhler A, Schluter A.** 2004. Antibiotic multiresistance plasmid pRSB101 isolated from a wastewater treatment plant is related to plasmids residing in phytopathogenic bacteria and carries eight different resistance determinants including a multidrug transport system. Microbiology **150:**3613–3630. http://dx.doi.org/10.1099/mic.0.27317-0.
27. **Minakhina S, Kholodii G, Mindlin S, Yurieva O, Nikiforov V.** 1999. Tn*5053* family transposons are res site hunters sensing plasmidal *res* sites occupied by cognate resolvases. Mol. Microbiol. **33:**1059–1068. http://dx.doi.org/10.1046/j.1365-2958.1999.01548.x.
28. **Kamali-Moghaddam M, Sundström L.** 2000. Transposon targeting determined by resolvase. FEMS Microbiol. Lett. **186:**55–59. http://dx.doi.org/10.1111/j.1574-6968.2000.tb09081.x.
29. **Petrovski S, Stanisich VA.** 2010. Tn*502* and Tn*512* are *res* site hunters that provide evidence of resolvase-independent transposition to random sites. J. Bacteriol. **192:**1865–1874. http://dx.doi.org/10.1128/JB.01322-09.
30. **Horak R, Kivisaar M.** 1999. Regulation of the transposase of Tn*4652* by the transposon-encoded protein TnpC. J. Bacteriol. **181:**6312–6318.
31. **Toleman MA, Biedenbach D, Bennett D, Jones RN, Timothy R, Walsh TR.** 2003. Genetic characterization of a novel metallo-β-lactamase gene, bla_{IMP-13}, harboured by a novel Tn*5051*-type transposon disseminating carbapenemase genes in Europe: report from the SENTRY worldwide antimicrobial surveillance programme. J. Antimicrob. Chemother. **52:**583–590. http://dx.doi.org/10.1093/jac/dkg410.
32. **Scotta C, Juan C, Cabot G, Oliver A, Lalucat J, Bennasar A, Alberti S.** 2011. Environmental microbiota represents a natural reservoir for dissemination of clinically relevant metallo-β-lactamases. Antimicrob. Agents Chemother. **55:**5376–5379. http://dx.doi.org/10.1128/AAC.00716-11.
33. **Lagatolla C, Edalucci E, Dolzani L, Riccio ML, De Luca F, Medessi E, Rossolini GM, Tonin EA.** 2006. Molecular evolution of metallo-β-lactamase-producing *Pseudomonas aeruginosa* in a nosocomial setting of high-level endemicity. J. Clin. Microbiol. **44:**2348–2353. http://dx.doi.org/10.1128/JCM.00258-06.